

Plasmon-induced dynamics of H₂ splitting on a silver atomic chain

Lei Yan, Zijiang Ding, Peng Song, Fangwei Wang, and Sheng Meng

Citation: [Applied Physics Letters](#) **107**, 083102 (2015); doi: 10.1063/1.4929611

View online: <http://dx.doi.org/10.1063/1.4929611>

View Table of Contents: <http://scitation.aip.org/content/aip/journal/apl/107/8?ver=pdfcov>

Published by the [AIP Publishing](#)

Articles you may be interested in

[Plasmon resonances in linear noble-metal chains](#)

J. Chem. Phys. **137**, 194307 (2012); 10.1063/1.4766360

[The dynamic effects on dissociation probability of H₂-Pt\(111\) system by embedded atom method](#)

J. Appl. Phys. **109**, 063509 (2011); 10.1063/1.3554690

[Dissociative dynamics of spin-triplet and spin-singlet O₂ on Ag\(100\)](#)

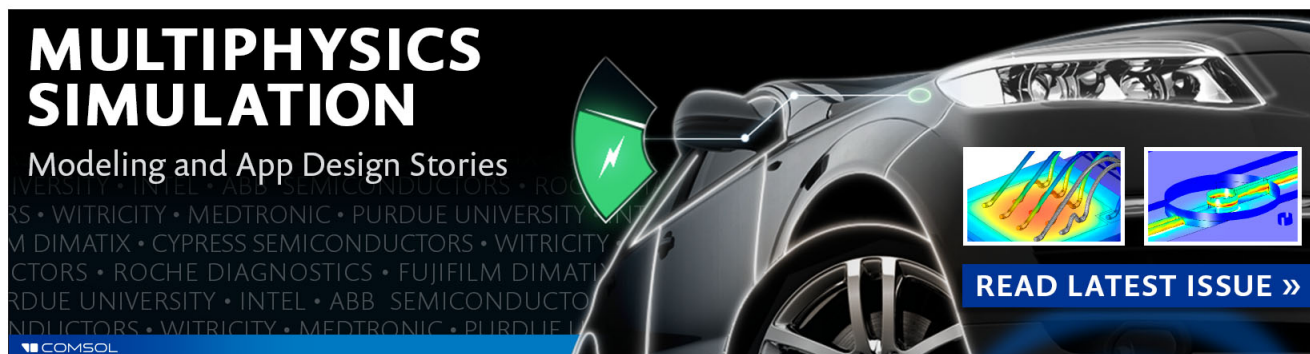
J. Chem. Phys. **129**, 224702 (2008); 10.1063/1.3012354

[High-sensitivity surface plasmon resonance spectroscopy based on a metal nanoslit array](#)

Appl. Phys. Lett. **88**, 243105 (2006); 10.1063/1.2209717

[Ultrafast dynamics of femtosecond laser-induced periodic surface pattern formation on metals](#)

Appl. Phys. Lett. **87**, 251914 (2005); 10.1063/1.2146067

The advertisement features a dark background with a car's front end on the right. On the left, the text 'MULTIPHYSICS SIMULATION' is written in large, bold, white letters. Below it, 'Modeling and App Design Stories' is written in a smaller white font. A green lightning bolt icon is positioned to the left of the car. Two small inset images show simulation results: one with a color gradient and another with a blue and yellow pattern. At the bottom left, the COMSOL logo is visible. At the bottom right, a blue button with white text says 'READ LATEST ISSUE >>'.

**MULTIPHYSICS
SIMULATION**

Modeling and App Design Stories

UNIVERSITY • INTEL • ABB SEMICONDUCTORS • ROCH
RS • WITRICITY • MEDTRONIC • PURDUE UNIVERSITY • IN
M DIMATIX • CYPRESS SEMICONDUCTORS • WITRICITY
CTORS • ROCHE DIAGNOSTICS • FUJIFILM DIMATI
RDUE UNIVERSITY • INTEL • ABB SEMICONDUCTO
NDUCTORS • WITRICITY • MEDTRONIC • PURDUE U

COMSOL

READ LATEST ISSUE >>

Plasmon-induced dynamics of H₂ splitting on a silver atomic chain

Lei Yan, Zijing Ding, Peng Song, Fangwei Wang, and Sheng Meng^{a)}

Beijing National Laboratory for Condensed Matter Physics and Institute of Physics, Chinese Academy of Sciences, Beijing 100190, China

(Received 16 June 2015; accepted 14 August 2015; published online 26 August 2015)

Localized surface plasmon resonances (LSPR) supported in metal nanostructures can be efficiently harnessed to drive photocatalytic reactions, whose atomic scale mechanism remains a challenge. Here, real-time dynamics of H₂ photosplitting on a linear silver atomic chain, upon exposure to femtosecond laser pulses, has been investigated using time-dependent density functional theory. The wavelength dependent H₂ splitting process is strongly coupled to LSPR excitation in silver chain. We identify that hot electrons produced in the silver chain by plasmon excitation are transferred to the antibonding state of the adsorbed H₂ and trigger H₂ dissociation, consistent with experimental observations. Increasing illumination intensity and the length of atomic chain promote H₂ splitting, thanks to stronger LSPR. Dynamic electronic response can be quantitatively described within the present approach, providing insights towards a complete fundamental understanding on plasmon-induced chemical reactions at the microscopic scale. © 2015 AIP Publishing LLC. [<http://dx.doi.org/10.1063/1.4929611>]

Collective electronic oscillation in metal nanostructures, also known as localized surface plasmon resonance (LSPR), exhibits extraordinary properties such as extended lifetime, tunable resonance energy, ultrafast dynamics, and enhanced optical absorption.^{1–4} Such properties of LSPR have fueled the development of novel applications including ultrasensitive biosensing,^{5,6} biomedical treatment,^{7,8} and catalytic chemical reactions.^{9,10} A variety of metal structures can be employed for such purposes. Prototype structures, which can be assembled with a scanning tunneling microscope (STM), include, for instance, linear atomic chains,^{11,12} artificial quantum dots,¹³ and quantum corrals.¹⁴ A unique advantage is that the size and shape of such structures are tunable down to the precision of a single atom. Collective electronic oscillation at such a scale is a fundamental subject of its own interest.¹⁵

Plasmon-enabled photochemistry has drawn great attentions due to its high throughput and low energy requirements. Among them, plasmon-induced H₂ splitting is one of the model reactions of fundamental importance. Mukherjee *et al.* presented first experimental evidences for room-temperature H₂ splitting on 5–30 nm gold nanoparticles supported on TiO₂¹⁶ and SiO₂¹⁷ under visible light illumination. They proposed that hot electrons, created from plasmon decaying, can be transferred into the closed shell H₂ molecules inducing H₂ dissociation. However, this proposal is highly speculative and has not been confirmed either in theory or experiment. Recently, Sil *et al.*¹⁸ optically detected gaseous hydrogen using assembled gold nano-hemispheres and demonstrated that dissociated hydrogen atoms form a metastable gold hydride. These studies open up a new route for low-temperature photoinduced chemical reactions on metallic catalysts. However, despite tremendous experimental studies, which probe the process indirectly and only report

macroscopic properties such as average reaction rates of HD formation, a microscopic picture of plasmon-induced H₂ splitting, especially the dynamic process, is still lacking.

Here, we investigate the atomic scale mechanism and real time dynamics of H₂ photosplitting on a silver atomic chain irradiated by femtosecond laser pulses (Fig. 1(a)), using *ab initio* time dependent density functional theory (TDDFT).¹⁹ We found that real-time H₂ splitting is enabled only at the resonance frequency of the LSPR in silver chain. Increasing laser intensity beyond a critical fluence would speed up H₂ photosplitting rate. By analyzing the dynamic charge distribution around H₂, we find hot electrons inject from the silver chain to the antibonding state of adsorbed H₂. This study provides a theoretical basis for understanding the microscopic mechanism of plasmon-induced molecular splitting.

First-principles calculations are performed with a real-space and real-time TDDFT code, OCTOPUS,²⁰ using Local Density Approximation (LDA) for the exchange correlation functional. The simulation zone is defined by assigning a sphere around each atom with a radius of 6 Å and a spacing of 0.3 Å between grid points. Hartwigsen-Goedecker-Hutter

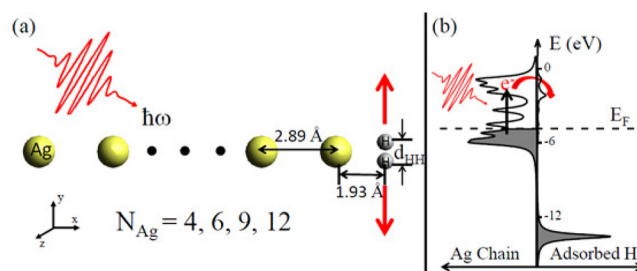


FIG. 1. (a) Schematic showing plasmon-induced H₂ splitting on Ag atomic chain with variable number of Ag atoms N_{Ag} . (b) Calculated electronic density of states (DOS) of H₂ approaching a linear chain of six silver atoms, localized on silver atoms (left panel) and H₂ (right panel). Horizontal dashed line denotes the Fermi level and grey regions refer to occupied electronic states.

^{a)} Author to whom correspondence should be addressed. Electronic mail: smeng@iphy.ac.cn

pseudopotentials are used to represent the interaction between valence electrons and the atomic core.²¹ Photoabsorption spectra are obtained by propagating the electronic density for a duration of 33 fs following an impulse excitation at time zero.^{22,23} To simulate the dynamics of H₂ photosplitting, Kohn-Sham wavefunctions of the Ag-H₂ system in a laser field are evolved for 20 000 steps with a time step of 0.003 fs. Time propagator is approximated by a fourth-order Taylor expansion in the Ehrenfest scheme for the electron-ion dynamics, with an initial temperature fluctuating around 300 K.

The geometry configuration of H₂ adsorbed on Ag atomic chain is shown in Fig. 1(a). In our simulation, Ag atoms in the chain are frozen with interatomic distance of 2.89 Å, chosen from the experimental value for Ag chains on NiAl(110) surface.²⁴ We select Ag chains with the number of atoms $N_{\text{Ag}} = 4, 6, 9, 12$ as models, which can be created by manipulating single Ag atoms on the NiAl(110) surface with a STM tip.²⁴

We first test the adsorption of H₂ molecule on the Ag chain, taking $N_{\text{Ag}} = 6$ as an example. H₂ was initially placed at a few representative high symmetry sites. After geometry relaxation the most stable structure is that with H₂ perpendicularly adsorbed at the end position with H-H facing the end Ag atom (shown in Fig. 1(a)). We note that in real experiments, the NiAl substrate has been used to stabilize the Ag chain;²⁴ thus, the optimal adsorption configuration of H₂ might be modified, thanks to the steric hindrance of the substrate.

We explore the optical absorption of silver atomic chain with variable length, shown in Fig. 2. These curves show a dominant peak at 2.15, 1.67, 1.28, and 1.03 eV for the chain with $N_{\text{Ag}} = 4, 6, 9, 12$, respectively. We note that the peak positions for plasmon excitation computed by TDDFT are strongly functional dependent.^{25,26} Compared with experimental results, LDA functional underestimates the plasmon energy by ~ 0.1 eV.²⁷ However, as we focus here on the dynamic aspect of the plasmon-molecule system, the quantitative difference in plasmon energy is not important. This major peak comes from dipolar plasmon excitation. As the length of Ag chain increases, oscillator strengths increase as a result of the accumulation of free electrons in the chain, and resonance frequency redshifts. Therefore, plasmon excitation energy can be tuned in a large range from 1.03 eV

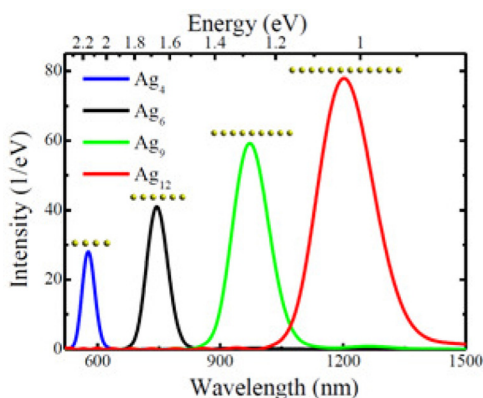


FIG. 2. Optical absorption spectrum of a linear Ag chain with $N_{\text{Ag}} = 4, 6, 9, 12$.

(corresponding to light wavelength of 1202 nm) to 2.15 eV (577 nm), covering the visible and infrared region.^{28,29} After H₂ adsorbed at the end of chain, the resonance frequencies are slightly greater than that in Fig. 2. For example, the peak energy blueshifts to 1.74 eV for $N_{\text{Ag}} = 6$.

Femtosecond laser pulses provide a powerful tool to engineer electronic excitations and to study the ultrafast dynamics of chemical reactions.³⁰ Here, we model the laser pulse field polarized in the x direction along the chain by a Gaussian wave packet (Fig. 3(a))

$$E(\omega, t) = E_{\text{max}} \exp\left[-\frac{(t-t_0)^2}{2\tau^2}\right] \cos(\omega t - \omega t_0 + \varphi) \quad (1)$$

to mimic the experimental set-up in Ref. 31. For simplicity, phase φ is set to zero and the width τ of the pulse is 10 fs. At the time $t_0 = 33$ fs, laser field reaches the maximum intensity E_{max} .

Next, we test the response of Ag-H₂ system to the external laser pulse applied. We find that with the strength of laser field gradually increasing in time, H-H bond length in Ag-H₂ system oscillates periodically and gradually deviates from its original value of 0.74 Å. For the system under a laser pulse with E_{max} of 2.5 V/Å and frequency $\hbar\omega = 1.74$ eV, we find that the period for H₂ oscillation is 9.3 fs, longer than 7.5 fs for H₂ in vacuum. Under laser excitation, the vibration slows down, and more importantly, the bond length keeps increasing from $d_{\text{HH}} = 0.94$ Å at $t = 30$ fs to $d_{\text{HH}} = 2.72$ Å at $t = 66$ fs (Fig. 3(b) black line). Under the same condition, an isolated H₂ molecule in vacuum oscillates around its equilibrium value and never breaks up (Fig. 3(b) black dashed line). Therefore, we can exclude the possibility of direct

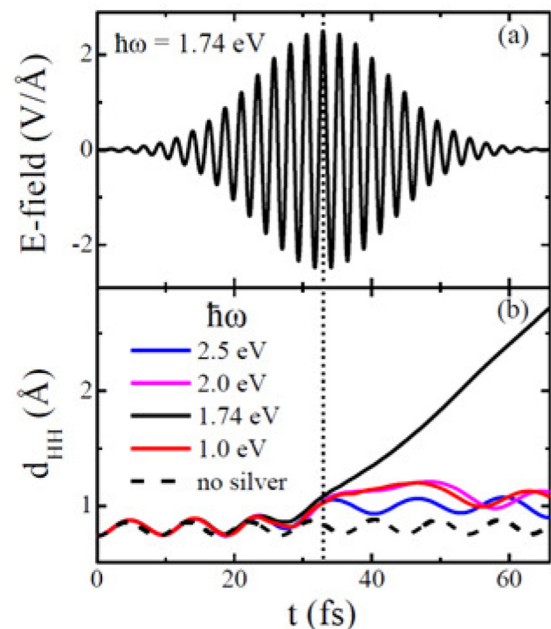


FIG. 3. (a) Time-dependent field strength of the laser pulse. The maximum amplitude E_{max} is 2.5 V/Å and laser frequency is 1.74 eV. (b) Time evolution of bond length d_{HH} under laser illumination with a maximum field strength $E_{\text{max}} = 2.5$ V/Å but different frequency. The dashed line is the case for isolated H₂ in vacuum with $\hbar\omega = 1.74$ eV. The vertical dotted line denotes the time at which laser field reaches its maximum strength.

photosplitting of H_2 , which requires the system to overcome the electronic excitation gap of 11.4 eV and atomic energy barrier of 4.6 eV.

A striking finding is the plasmonic enhancement of H_2 photosplitting on the Ag chain. In the following, we deem the H_2 molecule is split if the bond length d_{HH} is greater than 1.5 Å. Laser field in the same strength of $E_{\max} = 2.5 \text{ V/Å}$ is used to drive H_2 dissociation. With the laser frequency of $\hbar\omega = 1.74 \text{ eV}$, the dissociation of H_2 is obvious (see Fig. 3). While for other frequencies such as $\hbar\omega = 1.0 \text{ eV}$, 2.0 eV, and 2.5 eV, no dissociation is observed up to $t = 66 \text{ fs}$, despite that H_2 is distorted with oscillating period of 12.4 fs and the maximum bond length reaches 1.2 Å. Therefore, H_2 splits only when the laser frequency equals the LSPR frequency of the Ag atomic chain, namely, only when the LSPR of Ag chain is excited.^{32–34}

The H_2 splitting dynamics also exhibits dependence on the field strength or intensity of laser pulse. This is demonstrated in Fig. 4(a) with a fixed laser frequency $\hbar\omega = 1.74 \text{ eV}$. Before $t = 20 \text{ fs}$, the H-H bond oscillation for different laser intensity is identical. After $t = 20 \text{ fs}$, with E_{\max} varying from 0.05, 1.0, to 2.0 V/Å, the frequency of hydrogen stretching slows down and the maximum bond length d_{HH} increases to 0.87, 0.93, 1.14 Å, respectively. When E_{\max} reaches 2.5 V/Å, bond length keeps increasing linearly from 0.94 Å at $t = 30 \text{ fs}$ to 2.42 Å at $t = 60 \text{ fs}$. If we further increase the intensity to 3.0 V/Å, d_{HH} reaches 6.69 Å at $t = 60 \text{ fs}$, showing enhanced H_2 splitting behavior in stronger laser field. Therefore, there exists a critical field amplitude $E_c = 2.5 \text{ V/Å}$. Only when laser field strength is larger than the critical value E_c , H_2 molecule can split within 50 fs. Furthermore, by varying laser width τ in the time scale between 3.3 and 13.2 fs with fixed $\hbar\omega = 1.74 \text{ eV}$ and $E_{\max} = 3 \text{ V/Å}$, we find H_2 dissociation happens if τ is greater than 6.58 fs (Fig. S1).³⁵ Both parameters E_{\max} and τ can be integrated to produce laser fluence F . Therefore, a critical fluence $F_c = 0.72 \text{ J/cm}^2$ is found to enable H_2 photosplitting on Ag_6 atomic chain for the laser frequency of $\hbar\omega = 1.74 \text{ eV}$.

To understand the intensity dependence of plasmon-induced H_2 splitting, we analyze the dynamic charge transfer from Ag atomic chains to bound H_2 molecule upon laser excitation. Figure 4(b) shows the calculated charge around H_2 denoted as Q_{HH} for real-time tracking. Here, Q_{HH} is obtained by integrating total charge density above the plane between H_2 and Ag chain, which is vertical to the Ag chain and stands 0.8 Å away from the end Ag atom. The Q_{HH} is initially 2.0 e for all the cases. At $t = 20 \text{ fs}$, it increases to 1.92 and 2.17 e for E_{\max} in 0.05 and 1.0 V/Å, respectively; however, for $E_{\max} > 2.0 \text{ V/Å}$, Q_{HH} turns into 2.5–2.8 e , namely, about additional 0.5–0.8 e is transferred from Ag chain to H_2 . The amount of charge transfer might be underestimated, due to electron loss after transfer to the absorbing boundary applied to avoid spurious reflection at the grid boundary.³⁶ This is also evidenced by electron ionization process after 40 fs, thanks to the strong external field. Electron ionization could also be overestimated considerably due to the incorrect asymptotic behavior of the LDA Kohn-Sham potential. The increase in Q_{HH} by 0.5–0.8 e at $t = 20 \text{ fs}$ results in a transient negative H_2^- state and subsequent H_2 splitting dynamics. Weak field below E_c does not provide enough energy for hot electrons to overcome the energy barrier for charge transfer; thus, no hot electron transfers and no H_2^- forms.

To unravel the atomistic mechanism for plasmon-driven H_2 dissociation, we calculate localized electronic density of states (LDOS) of H_2 molecule and Ag atoms in the chain with $N_{Ag} = 6$ (Fig. 1(b)). One expects that electrons in the chain are initially optically excited. Then, hot electrons generated by plasmon decay transfer into the antibonding orbital of H_2 , forming transient negative ion H_2^- . The H_2^- travels on the excited state potential surface, extends its bond length, overcomes the activation barrier, and splits. We also note that the Ehrenfest dynamics is a good approach for systems where ions move on a coherent superposition of similar potential energy surfaces.³⁷ When these potential energy surfaces are dissimilar, trajectory surface hopping may be more reliable for simulations of nonadiabatic dynamics.

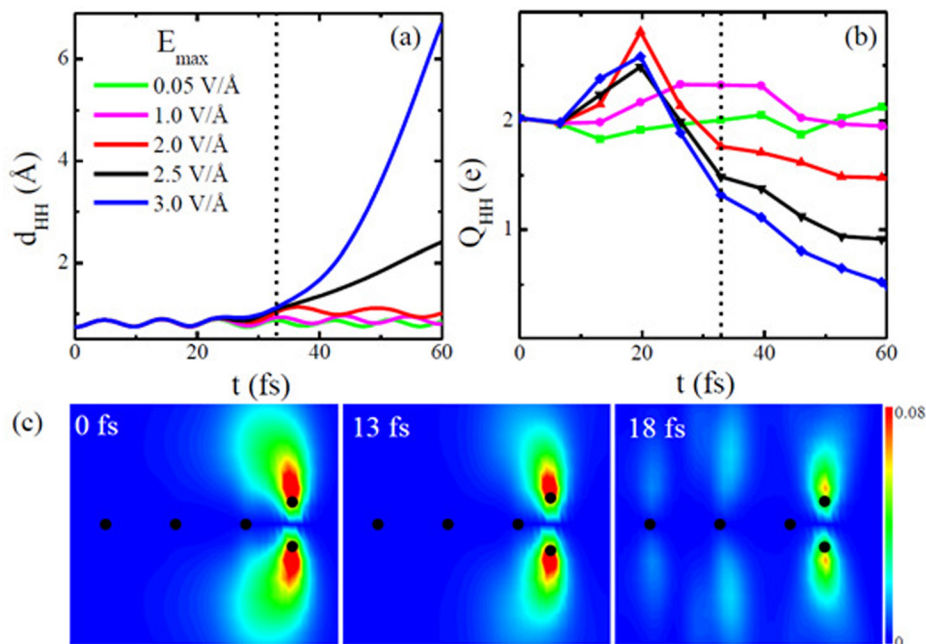


FIG. 4. Time evolution of d_{HH} (a) and charge around H_2 Q_{HH} (b) for the same frequency $\hbar\omega = 1.74 \text{ eV}$, setting E_{\max} as 0.05, 1.0, 2.0, 2.5, and 3.0 V/Å. These values of E_{\max} give the laser fluences of 0.29, 116.13, 464.52, 725.81, and 1045.16 mJ/cm^2 , respectively. (c) Snapshots for the charge density on the $z = 0$ plane in the antibonding state of the adsorbed H_2 . The unit of scale is 37.04 Å^{-3} .

To confirm that hot electrons are transferred to the antibonding state of absorbed H_2 , we show in Fig. 4(c) time evolution of charge density in the empty antibonding state. Initially, charge density is mainly localized on the antibonding orbital of the H_2 molecule (0 fs). At $t = 13$ fs, electron density around H_2 decreases, and delocalizes over H_2 and Ag chain. As time evolves to $t = 18$ fs, most charge density is shared between H_2 and Ag chain. This indicates the antibonding state of H_2 mixes with filled states on the Ag chain. In other words, a fraction of electrons in the filled state would transfer to the antibonding orbital of absorbed H_2 to preserve orthogonality of states. Projection of the time-dependent KS states on the anti-bonding eigenstate of H_2 shows that the antibonding state is partially occupied and the occupation is increasing during the dynamic evolution (Fig. S2).³⁵ From the time-dependent Kohn-Sham eigenvalues (Fig. S3),³⁵ the occupied orbitals are indeed overlapped with the antibonding orbital of H_2 in the time range of 10–20 fs, when charge transfer takes place (Fig. 4(b)). We emphasize that there are sufficient couplings between the high-energy Ag states and H_2 antibonding state during the dynamic evolution after plasmonic excitation. Therefore, the laser pulse drives electrons to the excited states, which then couple to the antibonding state of H_2 facilitating dynamic electron transfer. This result is in general accordance with the mechanism speculated for plasmon-induced photochemistry reactions.^{16,17,38}

In order to test the universality of our finding, we also explore the dependence of H_2 dissociation dynamics on the length of the atomic chain. As more Ag atoms are added to the chain, different evolution of H_2 is observed in Fig. 5. Under the same illumination laser fluence 0.46 J/cm^2 , the system for $N_{\text{Ag}} = 4, 6, 9, 12$ is resonantly excited by the laser with the frequency $\hbar\omega = 2.26, 1.74, 1.31, 1.05 \text{ eV}$, respectively. After the illumination, the H_2 oscillation period increases from 9.3 fs to 10.74, 14.74, and 33.5 fs, and the maximum d_{HH} to 0.99, 1.14, and 1.31 \AA , for $N_{\text{Ag}} = 4, 6, 9$, respectively. While for $N_{\text{Ag}} = 12$, d_{HH} reaches 1.56 \AA and H_2 splits directly. With the laser pulse resonant with the plasmon of Ag chain, H_2 dissociation is accelerated on the longer chain under the same illumination fluence.

In addition, the critical laser fluence F_c for H_2 dissociation on the silver chain with varied length is shown in Fig. 5(b). Critical fluence F_c is found to be 0.79, 0.73, 0.61, and 0.46 J/cm^2 for $N_{\text{Ag}} = 4, 6, 9, 12$, respectively. Although

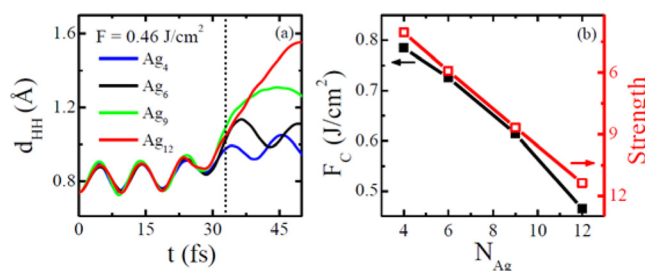


FIG. 5. (a) Bond length d_{HH} as a function of time for varied chain length under the same laser fluence 0.46 J/cm^2 with corresponding resonance frequency. (b) Critical laser fluence F_c (solid) for H_2 dissociation with $N_{\text{Ag}} = 4, 6, 9, 12$ and absorption strength (hollow) obtained from the absorption spectrum in Fig. 2.

Murdoch *et al.*¹⁰ demonstrate higher reaction rates on smaller Au nanoparticles with a diameter of 3–12 nm due to geometric effects, here we found that the increase of the H_2 dissociation rate on longer silver chains is most likely due to an electronic effect of silver chains in the length ranging from 1–4 nm. To test our proposal, we also show the oscillator strengths of silver chains in Fig. 5(b). LSPR can produce the strong near-fields that result in dramatic field enhancement, which facilitates subsequent electron transfer to H_2 . We estimated the local field enhancement at the H_2 position upon laser illumination, where an enhancement factor f_{FE} of 1.42, 1.94, 2.02, and 2.18 is found for the four cases. We found that the local field is enhanced to roughly the same value under corresponding critical external field E_c . These results fit well with a simplified electron transfer model: $R = (N_e \times \omega) \exp(-(E_a - f_{\text{FE}} \times E_c \times d_0)/k_{\text{B}}T)$, where R is the reaction rate for H_2 splitting, and N_e is the number of available electrons. E_a is the energy barrier between the Fermi level and the antibonding orbital of H_2 , which is taken as 2.52, 2.69, 2.80, and 2.84 eV for $N_{\text{Ag}} = 4, 6, 9, 12$, respectively. $d_0 \sim 0.5 \text{ \AA}$ is the effective width of the charge transfer barrier, and $k_{\text{B}}T$ is set to 0.026 eV at $T = 300 \text{ K}$. Furthermore, the reaction rate R is 0.023, 0.025, 0.023, and 0.024 fs^{-1} for $N_{\text{Ag}} = 4, 6, 9, 12$, respectively. We found that the reaction rate R reaches roughly 0.02 fs^{-1} for the Ag chains under the laser illumination of critical fluence.

In conclusion, we demonstrate H_2 splitting dynamics on silver chains is wavelength and field strength dependent upon laser excitation, due to dynamic charge transfer from silver nanostructure to the antibonding orbital of H_2 . This may help us to understand and to optically control chemical reactions at ambient conditions by plasmonic excitations.

This work was financially supported by the “973” Project of China (No. 2012CB921403), NSFC (Grant Nos. 11290164 and 11222431), and “Strategic Priority Research Program B” of the CAS (No. XDB070301).

¹S. Nie and S. R. Emory, *Science* **275**, 1102 (1997).

²H. Xu, E. J. Bjerneld, M. Käll, and L. Börjesson, *Phys. Rev. Lett.* **83**, 4357 (1999).

³E. Prodan, C. Radloff, N. J. Halas, and P. Nordlander, *Science* **302**, 419 (2003).

⁴N. Fang, H. Lee, C. Sun, and X. Zhang, *Science* **308**, 534 (2005).

⁵C. Zhang, A. X. Yin, R. Jiang, J. Rong, L. Dong, T. Zhao, L. D. Sun, J. Wang, X. Chen, and C. H. Yan, *ACS Nano* **7**, 4561 (2013).

⁶R. A. Álvarez-Puebla, L. M. Liz-Marzán, and F. J. García de Abajo, *J. Phys. Chem. Lett.* **1**, 2428 (2010).

⁷Y. L. Luo, Y. S. Shiao, and Y. F. Huang, *ACS Nano* **5**, 7796 (2011).

⁸C. Loo, A. Lowery, N. J. Halas, J. L. West, and R. Drezek, *Nano Lett.* **5**, 709 (2005).

⁹S. Lincic, P. Christopher, and D. B. Ingram, *Nat. Mater.* **10**, 911 (2011).

¹⁰M. Murdoch, G. I. N. Waterhouse, M. A. Nadeem, J. B. Metson, M. A. Keane, R. F. Howe, J. Llorca, and H. Idriss, *Nat. Chem.* **3**, 489 (2011).

¹¹N. Nilius, T. M. Wallis, and W. Ho, *Science* **297**, 1853 (2002).

¹²T. M. Wallis, N. Nilius, and W. Ho, *Phys. Rev. Lett.* **89**, 236802 (2002).

¹³M. F. Crommie, C. P. Lutz, and D. M. Eigler, *Science* **262**, 218 (1993).

¹⁴G. V. Nazin, X. H. Qiu, and W. Ho, *Science* **302**, 77 (2003).

¹⁵R. Huber, F. Tauser, A. Brodschelm, M. Bichler, G. Abstreiter, and A. Leitner, *Nature (London)* **414**, 286 (2001).

¹⁶S. Mukherjee, F. Libisch, N. Large, O. Neumann, L. V. Brown, J. Cheng, J. B. Lassiter, E. A. Carter, P. Nordlander, and N. J. Halas, *Nano Lett.* **13**, 240 (2013).

¹⁷S. Mukherjee, L. Zhou, A. M. Goodman, N. Large, C. Ayala-Orozco, Y. Zhang, P. Nordlander, and N. J. Halas, *J. Am. Chem. Soc.* **136**, 64 (2014).

- ¹⁸D. Sil, K. D. Gilroy, A. Niaux, A. Boulesbaa, S. Neretina, and E. Borguet, *ACS Nano* **8**, 7755 (2014).
- ¹⁹E. Runge and E. K. U. Gross, *Phys. Rev. Lett.* **52**, 997 (1984).
- ²⁰A. Castro, H. Appel, M. Oliveira, C. A. Rozzi, X. Andrade, F. Lorenzen, M. A. L. Marques, E. K. U. Gross, and A. Rubio, *Phys. Status Solidi B* **243**, 2465 (2006).
- ²¹N. Troullier and J. L. Martins, *Phys. Rev. B* **43**, 1993 (1991).
- ²²K. Yabana and G. F. Bertsch, *Phys. Rev. B* **54**, 4484 (1996).
- ²³A. Castro, M. A. L. Marques, and A. Rubio, *J. Chem. Phys.* **121**, 3425 (2004).
- ²⁴G. V. Nazin, X. H. Qiu, and W. Ho, *Phys. Rev. Lett.* **90**, 216110 (2003).
- ²⁵V. Kulkarni, E. Prodan, and P. Nordlander, *Nano Lett.* **13**, 5873 (2013).
- ²⁶C. M. Aikens, *J. Phys. Chem. A* **113**, 10811 (2009).
- ²⁷L. Jensen, L. L. Zhao, and G. C. Schatz, *J. Phys. Chem. C* **111**, 4756 (2007).
- ²⁸J. Yan, Z. Yuan, and S. Gao, *Phys. Rev. Lett.* **98**, 216602 (2007).
- ²⁹J. Yan and S. Gao, *Phys. Rev. B* **78**, 235413 (2008).
- ³⁰M. Lupetti, J. Hengster, T. Uphues, and A. Scrinzi, *Phys. Rev. Lett.* **113**, 113903 (2014).
- ³¹M. Lenner, A. Kaplan, C. Huchon, and R. E. Palmer, *Phys. Rev. B* **79**, 184105 (2009).
- ³²J. K. Matthew, A. Talin, and C. Phillip, *ACS Catal.* **4**, 116 (2014).
- ³³G. Toker, A. Bespaly, L. Zilberberg, and M. Asscher, *Nano Lett.* **15**, 936 (2015).
- ³⁴E. S. Thrall, A. P. Steinberg, X. Wu, and L. E. Brus, *J. Phys. Chem. C* **117**, 26238 (2013).
- ³⁵See supplementary material at <http://dx.doi.org/10.1063/1.4929611> for plasmon-induced dynamics of H₂ splitting on a silver atomic chain.
- ³⁶A. Castro, E. Räsänen, A. Rubio, and E. K. U. Gross, *Euro. Phys. Lett.* **87**, 53001 (2009).
- ³⁷O. V. Prezhdo and P. J. Rossky, *J. Chem. Phys.* **107**, 825 (1997).
- ³⁸M. J. Kale, T. Avanesian, H. Xin, J. Yan, and P. Christopher, *Nano Lett.* **14**, 5405 (2014).